BUTTERWORTH HEINEMANN

Polymer Vol. 36 No. 18, pp. 3555–3564, 1995

0032-3861/95/$10.00+0.00

Effects of soft segment prepolymer functionality on structure development in RIM copolymers

John L. Stanford, Richard H. Still and Arthur N. Wilkinson*
Manchester Materials Science Centre, University of Manchester and UMIST, Grosvenor Street, Manchester M1 7HS, UK
(Received 13 May 1994)

Segmented copolyureas and copoly(urethane-urea)s comprising 50% by weight of polyurea hard segments (HS) and polyether soft segments (SS) with different functionalities, have been formed by reaction injection moulding (RIM). The HS were formed from 4,4′-diphenylmethane diisocyanate reacted with mixed isomers of 3,5-diethyltoluene diamine. The nominal functionality of the SS prepolymers used (either amino- or hydroxyl-functionalized polyoxypropylenes with a constant molar mass per functional group of $\sim 2000\,g\,mol^{-1}$) was systematically increased from 2 to 4. RIM materials were characterized using a simple demould toughness test, and d.s.c. and d.m.t.a. were used to obtain SS and HS glass transition temperatures, T_g^S and T_g^H, and the degree of phase separation. Variations in the development of copolymer molar mass and HS sequence length, resulting from reactivity differences between the monomers and increasing functionality of the SS prepolymer, have been modelled using a statistical analysis of the RIM copolymerization. Schematic phase diagrams are presented, to aid interpretation of the complex effects of SS structure on the kinetic competition between polymerization and phase separation processes during the formation of RIM copolymers.

(Keywords: reaction injection moulding; polyurethane-urea; phase separation)

INTRODUCTION

Copoly(urethane-urea)s (PUU) and copolyureas (PUr) formed by reaction injection moulding (RIM)[1] are used extensively for large, complex components. These RIM copolymers are segmented block copolymers formed via random-step reactions of mixtures of (hydroxyl- or amine-) functionalized polyethers and aromatic diamines with aromatic diisocyanates[2]. However, during reaction to form the copolymers, as the liquid reactants are rapidly converted to a solid, a combination of spinodal decomposition-induced phase separation[3,4] and vitrification effectively quenches the system to yield a mixture of reaction products, comprising homopolymers, various AB-type block copolymers and free monomers[5]. This solid mixture possesses a non-equilibrium morphology[6–9] which arises from the direct competition between homo- and copolymerization kinetics, and thermodynamic changes occurring during the RIM process. Extensive studies[3,4,7–11] have shown that such a morphology comprises co-continuous soft- and hard-segment phases, the degree of phase separation of which depends on hard segment (HS) content, thermal history and HS structure.

The effects of soft segment (SS) prepolymer molecular structure on phase separation[12] are also important in determining copolymer morphology and properties. Varying the chemical structure of the SS changes its solubility parameter[12–14] and hence compatibility between soft and hard segments. In addition, increasing SS prepolymer molar mass at constant functionality (i.e. increasing the molar mass per functional group or equivalent weight, E_n) results[15–22] in a higher degree of phase separation, again due to increased incompatibility between the two copolymer segments. However, only limited studies have been published[22–24] on the effects of varying the functionality of the SS prepolymer in RIM copolymer systems. These papers indicate that increased SS prepolymer functionality results in reduced mould residence (or 'cure') time prior to demoulding and higher 'green strength' upon demoulding, but reduced flow-path length prior to vitrification, or 'flowability'[22].

SS prepolymers utilized in RIM are usually di- or tri-functional polyoxypropylenes with molar mass per functional group (equivalent weight, E_n) in the range $1000–2000\,g\,mol^{-1}$, which, in order to increase their reactivity, are either end-capped with 10–25% polyoxyethylene to give primary-hydroxyl tipped polyols, or the terminal hydroxyl groups are converted to amine groups. This paper reports on the effects of varying the functionality of SS prepolymers, with constant E_n, on the structural development of both RIM-PUU and RIM-PUr copolymers. The resulting variations in copolymer molar mass and microphase separation, and

* To whom correspondence should be addressed. Present address: Department of Materials Technology, Manchester Metropolitan University, John Dalton Building, Chester Street, Manchester M1 5GD, UK

their effects on RIM copolymer demould strength and thermal behaviour, are presented.

EXPERIMENTAL

Reactants

The materials formed in this study comprised up to four components: (i) a polyisocyanate; (ii) a polyether prepolymer with $E_n \sim 2000\,g\,mol^{-1}$; (iii) an aromatic diamine chain extender; and (iv) a catalyst for the hydroxyl-isocyanate reaction. The chemical structures of the various reactants are shown in *Scheme 1*.

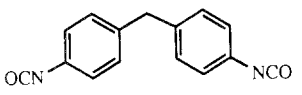

I

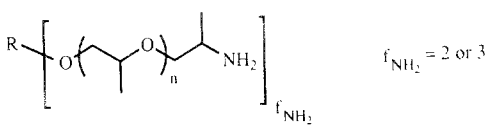

IIa

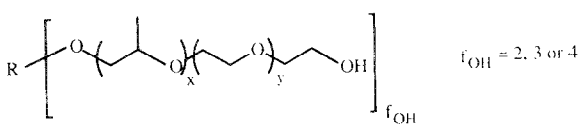

IIb

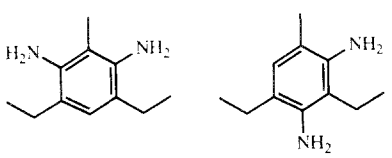

III

Scheme 1 Idealized reactant structures

The polyisocyanate, **I**, Isonate M340 (Dow Chemical), is a mixed uretonimine/urethane-modified variant of 4,4′-diphenylmethane diisocyanate (MDI) with a value of $E_n = 143 \pm 2\,g\,mol^{-1}$ by isocyanate titration[25], and a nominal functionality of 2.15.

The five polyethers are: amine-functionalized polyoxypropylenes, **IIa**, D4000 diamine and T5000 triamine (both Texaco Chemical); and hydroxy-functionalized poly(oxypropylene-oxyethylene)s, **IIb**, DS25 diol (ARCO), M111 triol (Lankro Chemical) and P1 tetrol (Union Carbide Chemical). The polyols are block copolymers comprising ~ 80–85 mol % of oxypropylene end-capped with ~ 20–15 mol % of oxyethylene. The E_n of each of the five prepolymers was determined by acetylation[26]: potentiometric amine titration[27] was also used to characterize the polyamines. G.p.c. was used to determine average molar masses for the three polyols, relative to polyoxyethylene standards[28].

The aromatic diamine chain extender, DETDA, **III**, is an 80:20 mixture of the 2,4- and 2,6- isomers of 3,5-diethyltoluene diamine (Lonza AG). The PUU systems contained dibutyltin-dilaurate, at a concentration of 1.05 mol/mol isocyanate groups, to catalyse the hydroxyl-isocyanate reaction. The reactants were used as-received, without further purification.

Reaction injection moulding

RIM materials were moulded as narrow rectangular plaques ($75 \times 250 \times 3.5$ mm) using in-house RIM equipment that has been described in detail elsewhere[28]. The formulations and processing data are given in *Table 1*, where Q_p and Q_i are the machine throughputs used, respectively, for the polyisocyanate and the polyol/polyamine reactant streams, and μ_p and R_p are the viscosity and the Reynolds number, respectively of the polyol/polyamine reactant stream. All the materials were formulated to contain 50% by weight DETDA/MDI hard segments, and the stoichiometric ratio of isocyanate to total amine/hydroxyl groups used was 1.03. Reactant pressures of 3000 ± 50 p.s.i. and initial reactant temperatures of 35 and 40°C, for the polyisocyanate and polyol/polyamine respectively, were used throughout. The RIM copolymers produced are designated using a two-character code referring to the SS prepolymer used. For example, DS is a copoly(urethane-urea) formed using the polyether diol DS25.

The demould toughness of the copolymers was determined using an area-diagram approach[5,6] by producing narrow plaque mouldings at a series of mould temperatures between 50 and 120°C, and demould times (i.e. the time from the mould being filled to it being opened) between 5 and 1200 s. On demoulding, each plaque was immediately subjected to a 90° bend at its midpoint, and its response was classified as either very tough (no visual damage), tough (visual damage but no break) or brittle (broke on bending). Plaques that broke in the mould were classified as being very brittle. Samples for thermal analysis were taken from plaques demoulded after 60–100 s at typical mould temperatures of 70 and 120°C for RIM-PUU and PUr materials, respectively.

Differential scanning calorimetry (d.s.c.)

D.s.c. studies were performed on a DuPont 990 thermal analyser fitted with a DuPont 910 cell base and equipped with a 990 d.s.c. cell. Samples (12–15 mg) and an inert reference material, 10 mesh glass beads (13 mg), were encapsulated in aluminium pans and cooled rapidly

Table 1 Formulations and processing details used to produce RIM copolymers

	DS25	M111	P1	D4000	T5000
M340[a]	208	209	206	209	207
Prepolymer[a]	265	264	267	263	265
DETDA[a]	100	100	100	100	100
Q_i(g s^{-1})	70.1	69.3	67.7	69.1	67.7
Q_p(g s^{-1})	123.3	121.3	121.0	120.0	119.1
μ_p(Pa s)[b]	0.30	0.34	0.42	0.26	0.28
R_p	1038	908	734	1182	1093

[a] The numbers in the table represent the parts by weight of reactants used in formulations

[b] Viscosity values were obtained at 50°C which includes the temperature rise (11 ± 2°C) in the reactant stream arising from viscous dissipation[28]

to −120°C in the cell. The sample and reference were subjected to a 20°C min^{-1} ramp rate in static air to 350°C. The glass transition temperatures were obtained from the d.s.c. traces as the intersection of tangents drawn to the onset baseline and the endothermic slope.

The degree of phase separation for each copolymer studied was obtained using the method of Camberlin and Pascault[29]. Thus the heat capacity change, ΔC_p^S, at the soft segment glass transition, T_g^S, was measured and compared to ΔC_p^{SO}, the heat capacity change of the pure soft segment material. The hard segment fraction of the material was known and the phase separation ratio (PSR) was established as reported previously[7–11].

Dynamic mechanical thermal analysis (d.m.t.a.)

D.m.t.a. data were obtained in the range −100 to 300°C using a Polymer Laboratories apparatus operating at a frequency of 1 Hz and a heating rate of 5°C min^{-1}. A double cantilever bending geometry was used for beam samples (3 × 10 × 45 mm) to obtain dynamic flexural moduli and mechanical damping as functions of temperature.

RESULTS AND DISCUSSION

Characterization and reactants

The values of E_n in *Table 2* obtained from acetylation, which is quantitative towards hydroxyl and amine groups, are similar for the various prepolymers, varying between ~ 1900 and ~ 2300 g mol^{-1}. The end-capped polyols used are known[1,31,32] to contain primary and secondary hydroxyl groups, with ~ 80% being primary. The number-average functionalities (f_n) of the polyols were determined from the ratio of number-average molar mass (from g.p.c.) to equivalent weight, and are given in the last column of *Table 2*. In the case of the triol and tetrol, the values of f_n are lower than the nominal values, 3 and 4 respectively. These differences are due to side reactions that occur during the base-catalysed propoxylation[24,31,33] yielding unreactive, unsaturated end groups. The main competing reaction involves the isomerization of propylene oxide into mono-functional allyl alcohol: subsequent reaction with propylene oxide results in the formation of allyl-terminated poly(oxypropylene) monols which reduce the overall functionality of the polyol.

The polyamines are known[34,35] to contain primary and secondary amino groups and residual secondary hydroxyls, with at least 85% of the total being primary amino groups. The characterization data in *Table 2* show the respective reactive groups of D4000 and T5000 to comprise 94 and 97% amino groups. End-group analysis[28,36] has found these groups to be almost exclusively primary amines, in agreement with published data[35]. G.p.c. analysis of phenyl-isocyanate capped T5000[36] reported an M_n value of ~ 6000 g mol^{-1}, indicating a functionality of 3.1 This close agreement with the nominal value of f_n may reflect some functionalization of unsaturated species under the conditions employed during amination[34].

Table 2 Characterization data for soft segment prepolymers

Prepolymer	E_n(g mol^{-1})[a]	E_n(g mol^{-1})[b]	M_n(g mol^{-1})[c]	f_n[d]
DS25 diol	2046 ± 19	—	4206	2.06
M111 triol	2182 ± 22	—	6066	2.78
P1 tetrol	2287 ± 23	—	7982	3.49
D4000 diamine	2167 ± 20	2304 ± 31	—	2[e]
T5000 triamine	1899 ± 10	1964 ± 20	—	3[e]

[a,b] E_n (the number-average molar mass per functional group) from, respectively, acetylation[26] and potentiometric titration[27]
[c] Number-average molar mass from g.p.c.
[d] Number-average functionality [$f_n = M_n$(g.p.c.)/E_n(acetylation)]
[e] Nominal functionality

Processing

The moulding area diagrams (MADs) for the RIM-PUU and RIM-PUr materials are shown in *Figures 1* and *2*, respectively. To aid discussion, curves have been drawn in both figures separating regions (in terms of mould temperature and demould time) relating to the classifications of the green strength of the RIM plaques, defined previously. The areas below the bottom curves define the very brittle (VB) regions where the plaques always fractured on opening the mould, as the material is incapable of sustaining even the moderate stresses arising from shrinkage due to polymerization and thermal

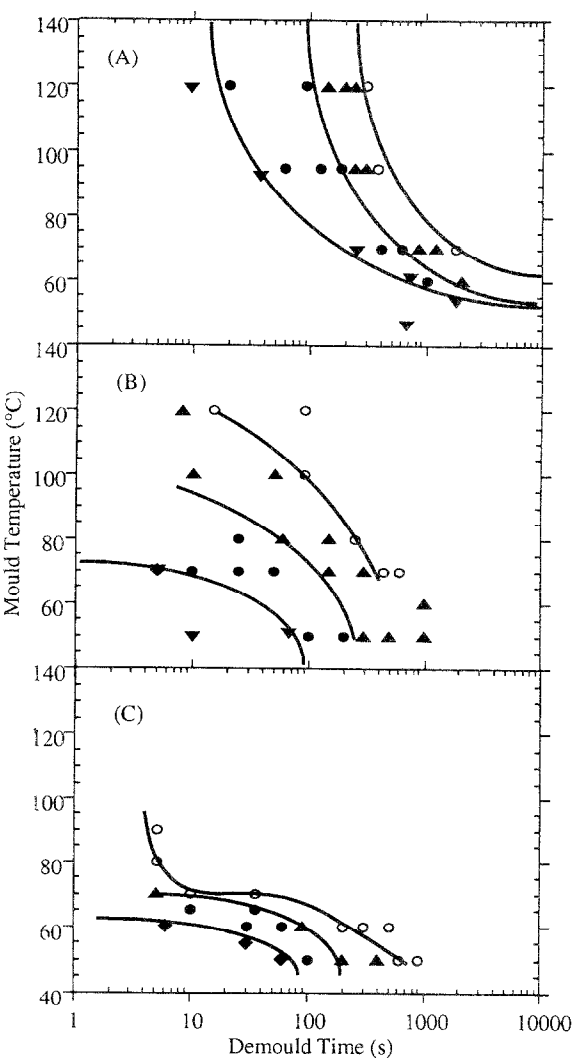

Figure 1 Demoulding area diagrams for (A) DS; (B) M1; and (C) P1 RIM-PUU systems: (▼) very brittle; (●) brittle; (▲) tough and (○) very tough materials

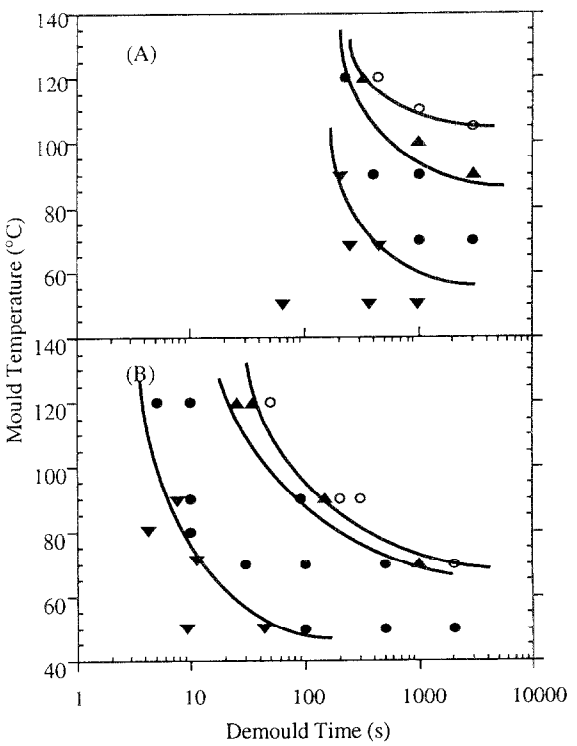

Figure 2 Demoulding area diagrams for (A) D4 and (B) T5 RIM-PUr systems: (▼) very brittle; (●) brittle; (▲) tough and (○) very tough materials

contraction. The middle curves define the transition regions from brittle (B) to tough (T) behaviour, in which complete plaques were demoulded, but when they were subjected to the 90° bend test they either fractured completely of suffered visible damage. Finally, the areas above the top curves define the very tough (VT) regions, where RIM plaques showed no visible damage after the 90° bend test. Generally, materials processed under relatively higher temperatures and/or longer times are usually capable of withstanding more severe stresses during demoulding. However in general industrial terms, mould temperatures of 100–120°C and demould times of 50–60 s may be regarded as upper limits for high speed RIM processing.

The changes of shape of the MADs reflect the differing functionality and chemical structure of the SS prepolymers. These molecular differences significantly affect the kinetics of copolymerization and the resulting morphologies, more detailed discussions of which are given in a later section. However, the MADs may also be discussed qualitatively in terms of SS prepolymer functionality and functional group structure (i.e. —OH vs. —NH_2). Thus, in the RIM-PUU systems (*Figure 1*) as the nominal functionality increases from 2 to 3 to 4, the area of the VB region decreases dramatically and the temperatures and times required to produce very tough materials are significantly reduced. For example, taking the point of comparison as 120°C mould temperature and 60 s demould time, the three copolymers exhibit significantly different green strengths (*Figure 1A–C*); DS is brittle, M1 is at the boundary of the T/VT regions and P1 is deep into the VT region. In fact, P1 exhibits VT behaviour after 60 s demould time at a mould temperature of 70°C, or after approximately 10 s at 100°C.

The RIM-PUr copolymers (*Figure 2*) exhibit similar trends in green strength upon increasing SS prepolymer functionality as in the PUU. However, the different functional group structure (i.e. —OH vs. —NH_2) results in significant differences in green strength development between the PUr and PUU systems, as shown by comparing the MADs for the bi-functional (A) and tri-functional (B) SS prepolymer systems in *Figures 1* and *2*. The PUr systems exhibit relatively small regions of VT behaviour, but the most significant differences are the reductions in the regions bounded by the B-to-T transition (i.e. the middle curve). These MADs confirm the requirement for different conditions when processing PUU and PUr systems[37]; i.e. higher mould temperatures (compare ~70°C with 120°C) are required to demould equivalent RIM-PUr materials without damage. For example, comparing the tri-functional systems (i.e. (*B*) in *Figures 1* and *2*) at 60 s demould time, the PUU material (M1) changes from B to T behaviour at ~80°C mould temperature and to VT at ~105°C, whereas the PUr material (T5) undergoes these changes at higher temperatures, namely ~100 and ~120°C respectively.

As expected, a more rapid development of demould toughness (green strength) results from the direct relationship between SS prepolymer functionality and copolymer molar mass development. Clearly, as the functionality of the SS prepolymer increases, the molar mass develops more rapidly (under given conditions), as do the mechanical properties of the RIM materials, exemplified in this study by the demould toughness. For example, comparing the behaviour of the three PUUs (*Figure 1*) at a mould temperature of 70°C, VT materials are produced after demould times of ~2000, 500 and 10 s upon increasing the nominal functionality from 2 to 3 to 4, respectively.

Differential scanning calorimetry (d.s.c.)

The d.s.c. data presented in *Table 3* show the trend in T_g^S values on progressing from unreacted prepolymers to isolated SS networks to phase separated copolymers. The table also allows comparison of the effects on T_g^S and PSR data of the different chemical structure of the functional group (i.e. —OH vs. —NH_2) and of the SS prepolymer functionality.

Reacting the SS prepolymers with M340 polyisocyanate to form an isolated polyether network results in a rise in T_g^S of ~5°C. This results from restrictions to molecular mobility of oxypropylene-oxyethylene units at the ends of soft segment chains attached to terminal hydroxyl or amine groups, which have subsequently reacted and been incorporated into the network. The greater potential for hydrogen bonding exhibited by urea groups compared to urethane groups results in a greater degree of association in the T5000-based network. This increased restriction to molecular mobility results in a higher value (~5°C) of T_g^S for the T5000 network, relative to the analogous M111-based network. Comparing the values of T_g^S of the networks with those of the RIM copolymers, only small increases (~2°C) are observed indicating that the SS phase responsible for the transition is relatively pure. In general, the value of T_g^S for both the SS prepolymers and RIM copolymers increased by ~5°C upon increasing the nominal SS prepolymer functionality from 2 to 3. This increase is indicative of a restriction of molecular mobility with

increasing functionality, but a further increase in functionality to 4 (P1 polyol) had no discernible effect upon values of T_g^S. In addition, replacing the poly(oxypropylene-oxyethylene) polyols with analogous polyoxypropylene polyamines had no effect on T_g^S within experimental error. No further transitions were observed by d.s.c. between T_g^S and the onset of thermal oxidative degradation at 250–300°C.

In *Table 3*, the value of PSR for each material is determined as the ratio of the heat capacity change of a RIM copolymer at T_g^S compared to that of the pure SS network, normalized for sample mass. The value of PSR is a measure of the fraction of SS which contributes to heat capacity at T_g^S and therefore does not include SS trapped either in the HS phase or the interphase regions.

Comparison of the PSR data (*Table 3*) for the PUU and PUr materials shows the latter to be more phase-mixed. This is in agreement with previously reported[4,8–11] PSR data for PUU and PUr materials, but is contrary to thermodynamic predictions[4,8,28] based on calculations of χ_{HS}/χ_C^L, the ratio of the hard segment/soft segment interaction parameter (derived from the solubility parameters[14]) to the critical interaction parameter, for the occurrence of microphase separation in a segmented block copolymer system[38,39]. The disagreement between prediction and experiment can be ascribed to the dynamic nature of the RIM process and the kinetic competition between copolymerization and microphase separation. The reactions which occur during the formation of RIM-PUr are much more rapid than those involved in the formation of RIM-PUU[40]. Therefore, vitrification occurs more rapidly in RIM-PUr, effectively quenching the system at a lower degree of microphase separation.

For both PUr and PUU, the value of PSR is observed to decrease significantly with increasing SS prepolymer functionality, which may be ascribed to the more rapid development of molar mass. The concomitant reduction in molecular mobility within the system will slow the rate of phase separation, relative to the rate of polymerization, and thus the system will be more phase-mixed at the onset of HS vitrification.

Dynamic mechanical thermal analysis

The curves in *Figures 3* and *4* show storage modulus (E') and damping (tan δ) vs. temperature data for the PUU and PUr materials, respectively. These curves are similar to those reported previously[3,4,7–11] for analogous phase-separated RIM copolymers, in that two major transitions are observed ascribed to the SS and HS glass transitions at temperatures T_g^S of approximately −40°C, and T_g^H in the range 180–250°C. In addition, the damping curves show a broad, low-intensity transition between 50 and 150°C, which is associated with the breakdown of hydrogen bonding between HS polyurea groups and the ether-oxygens of the SS. Detailed differences in values of T_g^S and T_g^H for the various PUU and PUr are given in *Table 4*.

The mechanical damping data show the value of T_g^S for the PUU (−42 ± 2°C) to be relatively insensitive to variations in SS functionality, and in good agreement with d.m.t.a. values of T_g^S of −40 ± 1°C for homogeneous polyurethane networks derived from M340 and either M111[21] or P1[30]. These observations indicate that the SS phases responsible for the low temperature

Table 3 D.s.c. and phase separation data for RIM copolymers

	T_g^S(°C)	PSR (%)
Copolymers		
DS	−68	81 ± 2
M1	−63	72 ± 4
P1	−64	66 ± 3
D4	−68	74 ± 2
T5	−62	68 ± 3
Networks		
M111/M340[a]	−66	—
P1/M340[b]	−65	—
T5000/M340[c]	−61	—
Prepolymers		
DS25	−74	—
M111	−70	—
P1	−70	—
D4000	−75	—
T5000	−68	—

[a,b,c] Data from references 21, 30 and 10, respectively
T_g^S derived from at least three traces for each material, typical 95% confidence limits (CL) ± 1°C
PSR data are averaged from at least nine determinations for each material and are shown ± 95% CL

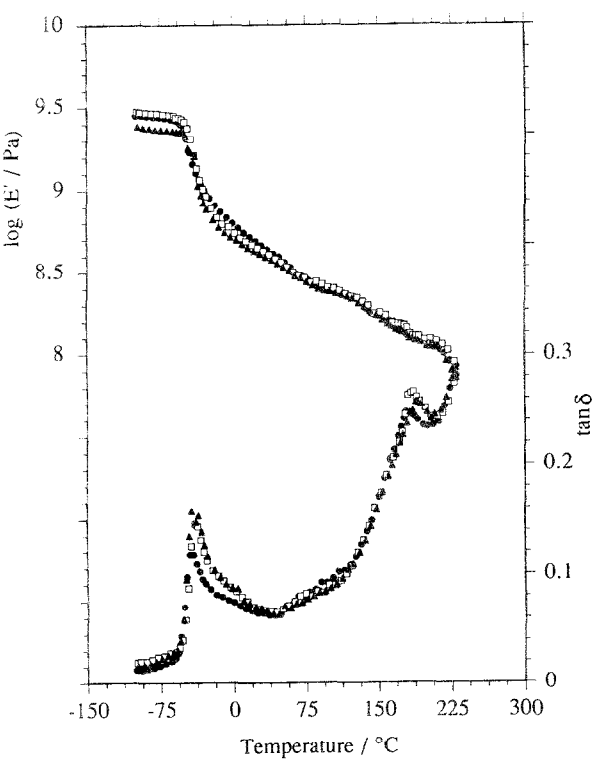

Figure 3 Dynamic flexural modulus (E') and mechanical damping (tan δ) at 1 Hz vs. temperature for copoly(urethane-urea)s: (●) DS; (□) M1 and (▲) P1

damping peaks are relatively pure. However, in all three materials the temperature range of the transition region is broad (approximately −60 to +45°C compared to −60 to 0°C for the M111- and P1-based networks[21,30]) indicating a significant degree of domain boundary mixing. The more phase-mixed M1 and P1 materials exhibit the broadest transitions, which is a result of the reduction in the rate of phase separation (with increasing SS prepolymer functionality) and the consequent onset of HS vitrification at a lower degree of phase separation. In general, similar low-temperature damping behaviour was observed for the PUr materials, albeit with slightly

Table 4 D.m.t.a. data for RIM copolymers

Copolymer	T_g^S(°C)	tan δ (T_g^S)	T_g^H(°C)	tan δ (T_g^H)	E'(−30°C)/E'(65°C)	E'(65°C)/E'(160°C)
DS	−44	0.138	184	0.255	2.6	2.0
M1	−40	0.155	188	0.268	3.0	2.1
P1	−41	0.168	194	0.266	3.2	2.0
D4	−37	0.136	243	0.368	3.2	1.7
T5	−34	0.120	238	0.339	4.1	1.8

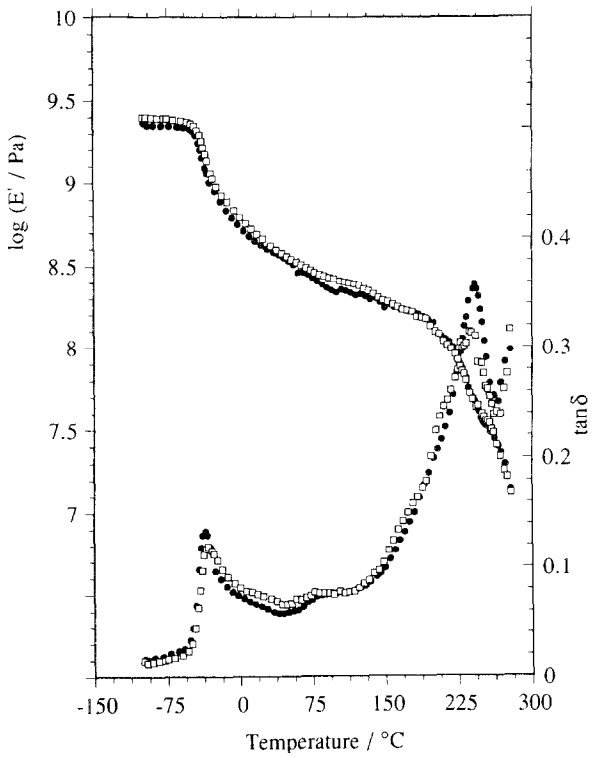

Figure 4 Dynamic flexural modulus (E') and mechanical damping (tan δ) at 1 Hz vs. temperature for copolyureas: (●) D4 and (□) T5

higher values of T_g^S and lower tan δ values than for the equivalent PUU, due to a greater degree of phase boundary mixing in these rapidly reacting systems. The degree of phase mixing is also observed to increase slightly with increasing SS functionality, as evidenced by a small increase in T_g^S and a broadening of the transition peak.

More significant differences between the two RIM copolymer systems are observed for values of T_g^H. The HS glass transition in the PUU materials is visible only as an ill-defined shoulder on a rising tan δ curve, whereas the PUr exhibit definite peaks of higher intensity at much higher temperatures (~240 compared to ~190°C), suggesting the presence of longer HS sequence lengths in these materials. This may be expected since the increased (~50°C) mould temperature, required to achieve PUr materials which can be demoulded without cracking, will delay vitrification of the HS and thus allow the development of longer sequence lengths. However, the requirement for higher mould temperatures itself indicates significant differences in the development of average HS sequence lengths, which will be discussed further in the following sections. In addition, it has been suggested[41] that the organo-tin polymerization catalysts incorporated into RIM-PUU systems may also promote depolymerization as the added catalyst has deleterious effects on the high-temperature properties of RIM-PUr[41]. Thus, it is also possible that the lower values of T_g^H observed for the PUU are due to the plasticizing effects of low molar mass degradation products.

The modulus–temperature dependence of the various RIM copolymers, expressed as the ratio of moduli at specified temperatures, is also given in *Table 4*. The ratio of moduli at −30 and 65°C is often quoted[1] as an indicator of the low temperature modulus–temperature behaviour of RIM copolymers. The magnitude of this ratio is dominated by the modulus change associated with the SS glass transition, the proximity of T_g^S to −30°C and the degree of phase mixing present in the material. Thus, the effect of segmental mixing may be observed in the variation of the ratio with SS functionality, such that DS < M1 < P1 and D4 < T5 (see *Table 4*), and the more phase-mixed PUr exhibit higher ratios than equivalent PUU. Modulus–temperature behaviour at higher temperatures is quantified over an equal temperature interval by the modulus ratio E'(65°C)/E'(160°C), which when compared to the E'(−30°C)/E'(65°C) ratios, are not only smaller but also show little dependence on SS functionality. For the PUU, the proximity of T_g^H to 160°C results in significantly higher values of this ratio than for equivalent PUr, which are known[41] to exhibit superior and prolonged, high-temperature dimensional stability.

Recursive-method calculations

In an attempt to gain a better understanding of the effects of SS prepolymer functionality on structure development during RIM copolymerizations, the growth of weight-average copolymer molar mass (M_w) and hard segment sequence length (N_w), as functions of isocyanate conversion (p) were modelled using recursive-method calculations[42]. This is a simple method for calculating the average molar masses of polymers without first determining their distributions, and has been applied to linear[40,43] and non-linear[28,44] RIM copolymerizations. The method utilizes the recursive nature of a step-copolymerization modelled as a first-order Markov chain process[45]. Thus, to determine weight-average molar mass in a typical three-component RIM system, a unit of each reactant is selected at random and the expected weight of the molecule, of which it is a part, is calculated; M_w is then obtained by averaging the weights of the three selected polymer molecules.

Recursive-method calculations were made[28] for three-component $RA_2 + RB_2 + RC_f$ systems (diisocyanate/chain extender/prepolymer), corresponding to a copolymer comprising 50% w/w DETDA/MDI HS and a SS

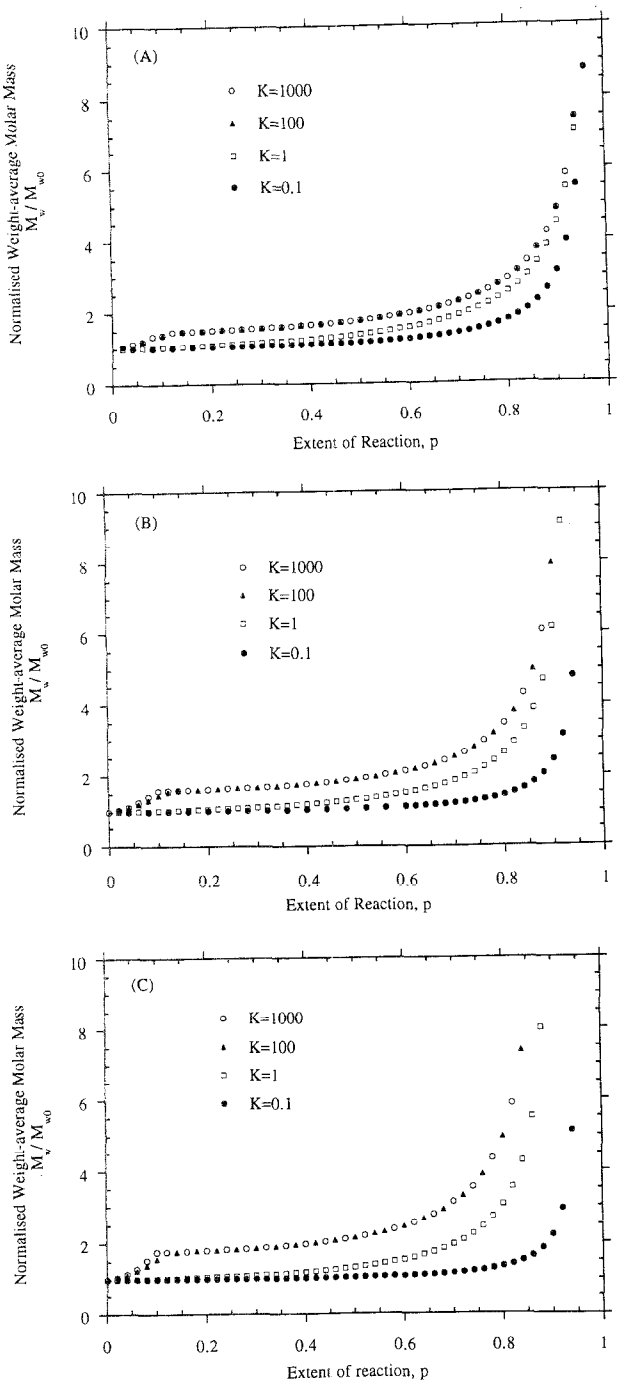

Figure 5 The development of relative weight-average molar mass as a function of isocyanate conversion (p) during RIM copolymerization. M_w data have been predicted by recursive-method calculations and normalized to M_{w0}, the initial value of M_w for the reaction mixture. The compositional parameters used in the model correspond to a 50% HS content system comprising MDI, DETDA and a SS prepolymer of 2000 g mol^{-1} equivalent weight, and a functionality of (A) 2, (B) 3 or (C) 4

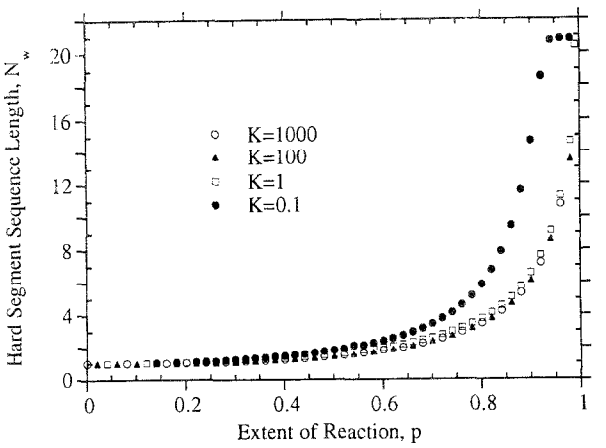

Figure 6 The development of weight-average HS sequence length (N_w) as a function of isocyanate conversion (p) during RIM copolymerization, as predicted by recursive-method calculations

prepolymer of $E_n = 2000\,g\,mol^{-1}$ and $f_n = 2$, 3 or 4. These results were coupled with a set of kinetic differential equations to introduce time dependence and unequal reactivity between the reactants[40,42,43]. Assumptions used in the modelling require that homogeneous reaction conditions exist, that all groups react independently of each other, that the diisocyanate and chain extender are di-functional and that the ratio, K, of the rate constants (isocyanate-SS:isocyanate-chain extender) is independent of temperature and conversion. As in previous studies[40,43], overall second-order kinetics were assumed, and the values of K used corresponded approximately to the degree of unequal reactivity expected during the formation of RIM-PUU (0.1–1.0) and PUr (100–1000). The kinetics equations were solved numerically to determine the conversion of each reactant as a function of time which, when coupled with the recursive-method calculations, allowed the calculation of M_w and N_w as functions of p as shown in *Figures 5A–C* and *6*, respectively.

To aid comparison, the molar mass data in *Figure 5* have been normalized to M_{w0}, the initial value of M_w for the reaction mixture, which is fixed for a given composition of reactants but increases with the functionality (and molar mass) of the SS prepolymer. When the reactivity of the SS prepolymer is high ($K = 1000$ or 100) the prepolymer is consumed during the early stages of the reaction (i.e. $0 \leqslant p \leqslant 0.1$), resulting in a sharp increase in M_w, as the prepolymer undergoes oligomerization and is capped with MDI. On increasing the functionality of the SS prepolymer from 2 to 4 (*Figure 5A–C*), the corresponding initial rise in M_w increases by 45 to 60 to 80% relative to M_{w0}, followed by a more rapid development of copolymer structure (and M_w) as the DETDA–MDI reaction proceeds. At lower values of K this sharp increase in M_w is not observed, and only a gradual increase in M_w/M_{w0} with p occurs and the rate of molar mass development increases with the value of K. For the non-linear systems, the conversions of isocyanate at gelation, p_g, were calculated using equation 1:

$$(rp_g)^2 = \frac{1}{(f_e - 1)(g_e - 1)} \qquad (1)$$

where r is the stoichiometric ratio and $f_e = \Sigma f_i^2 Af_i / \Sigma f_i Af_i$ is the weight-average functionality of a mixture of i various SS prepolymers and chain extenders with molar concentration Af_i; g_e is defined similarly for the isocyanates[1]. Using values of $f_n = 2$ for DETDA and MDI, and values of SS prepolymer f_n of 3 and 4, the levels of p_g were calculated to be 0.96 and 0.92, respectively. Values of p_g, calculated using experimental data for the materials described in *Table 1*, were $\geqslant 0.88$. Thus, since copolymerization is effectively quenched at a relatively early stage by the onset of HS vitrification,

chemical gelation is not envisaged to have occurred, although the network-forming reactions obviously have a significant effect on the development of M_w.

Variations of SS prepolymer functionality (at constant E_n) have no effect on the development of N_w during copolymerization; thus the recursive-method calculations generate only a single set of curves (*Figure 6*) at various values of K for the three theoretical systems. The limiting value of N_w, in this case 20.8, is dictated by the initial ratio of the three components. When the relative reactivity of the SS prepolymer is very low ($K = 0.1$), this limiting value is reached at $p = 0.96$, whereas for higher values of K, it is achieved only in the limit of complete reaction. The model therefore proposes that PUU copolymers contain longer HS sequence lengths than equivalent PUr, and should therefore exhibit higher values of T_g^H. However, the d.m.t.a. data in *Table 4* show the reverse trend to be the case. Furthermore, other studies[7–11] have found PUr materials to exhibit higher values of T_g^H than equivalent PUU. As discussed in the previous section, these differences may be artefacts resulting from thermal degradation, or may reflect genuine differences in the development of HS sequence lengths. One such difference is the high probability of phase separation occurring at a relatively early stage of PUU copolymerization. The advent of heterogeneous reaction conditions will slow the rate of reaction, causing N_w development to deviate significantly from the predictions of the copolymerization model.

Kinetic competition between copolymerization and microphase separation

During a RIM copolymerization, any significant changes in the growth of M_w and N_w, which may occur as a result of variations in SS functionality or unequal reactivity of the monomers, will also have dramatic effects on the development of structure as the system phase separates via spinodal decomposition[3,4]. This kinetic competition between copolymerization and phase separation in DETDA-based RIM copolymers is best described with the aid of schematic phase diagrams[4,9] as shown in *Figures 7a* and *b* for RIM-PUU and RIM-PUr systems, respectively. As they are purely aids to discussion, the figures have been drawn making two simplifying assumptions, namely that the coexistence curve is positioned symmetrically and that the process is assumed to be isothermal. Thus, the ordinate is defined only in terms of $1/\chi N$, the reciprocal product of the interaction parameter and the polymerization index, N. Superimposed on the phase diagram is a T_g vs. composition curve assuming complete reaction. The general behaviour of both PUU and PUr systems is similar in that initially the reactants are miscible and, under these homogeneous reaction conditions, copolymerization proceeds rapidly acting as a thermodynamic quench deep into the unstable region (represented by the vertical arrow through the critical point). Large values of N are quickly achieved, leading to the two-phase equilibrium position (Eq). The phase separation process (represented by the horizontal arrows) lags behind the reaction and is ultimately arrested by the vitrification of the HS-dominated phase, which attains a composition with T_g^H equivalent to the in-mould reaction temperature, T_{RIM}. This occurs at a position known as the Berghmans point[46] (shown as A′ and B′ in *Figures 7a* and *b*) and no further phase separation is possible. Thus, the values ϕ'_{RIM} and ϕ''_{RIM} define the composition of the final RIM material. In such phase diagrams, the interphase region is considered to be infinitesimally small. However, in real RIM materials a significant interphase will exist in which there is a gradual change in composition between the two dominant phases ϕ'_{RIM} and ϕ''_{RIM}.

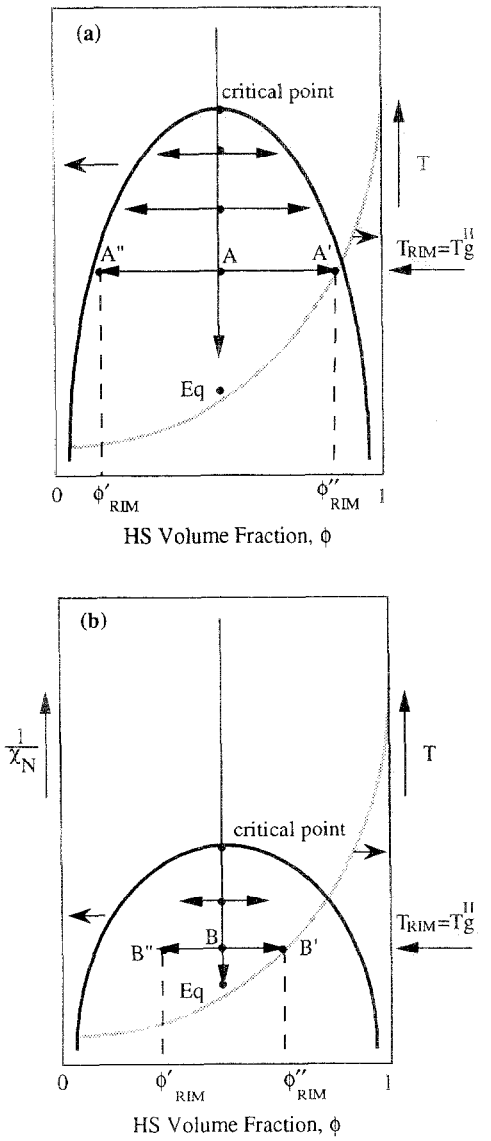

Figure 7 Schematic representation of the phase diagram coexistence curves (solid curves), superimposed with schematic T_g vs. composition curves (dotted curves), for (a) a system with low values of K, such as a PUU, and (b) a system with high values of K, such as a PUr. The vertical arrow through the critical point represents the extent of reaction of the system, and the horizontal arrows represent the degree of phase separation achieved as the reaction proceeds, relative to the maximum defined by the coexistence curve

The differences in phase development between the PUU and PUr systems are a result of the relative reactivities of the SS prepolymer and chain extender toward the diisocyanate (i.e. the values of the ratio K defined in the previous section). At low values of K, phase development is more like that in a mixture or blend; HS homopolymerization is the favoured reaction and macrophase separation of unconnected HS and SS chains occurs. For the 50% polyether/DETDA–MDI systems studied, comparison may be made between the calculated[28] driving force for microphase separation in a

segmented block copolymer, χ_{HS}/χ_C^L, and that for macrophase separation in a blend predicted by the Flory–Huggins relation[45], χ_{HS}/χ_C^{FH}, where χ_C^{FH} is the critical interaction parameter for the occurrence of macrophase separation in a polymer–polymer system[45]. Such a comparison shows the driving force for phase separation in a blend to be over three times greater than in a segmented block copolymer. Consequently, the coexistence curve for the RIM-PUU system has a higher critical point than for the RIM-PUr. This, coupled with the high degree of molecular mobility afforded by a blend-type system (due to a much lower initial viscosity and slow development of M_w), results in macrophase separation of nascent HS sequences at a relatively early stage in the polymerization, and rapid macrophase separation which almost keeps pace with polymerization until both processes are arrested by the onset of vitrification at the Berghmans point. Materials formed under these conditions exhibit coarse, highly phase-separated, co-continuous morphologies[4] but possess little strength due to the lack of interphase connectivity[9,17]. Commercial RIM-PUU formulations[1] consequently contain organo-tin catalysts to increase the rate of hydroxyl-isocyanate reactions, and to improve the demould toughness and ultimate mechanical properties of the material. When values of K are high, such as in RIM-PUr, the rapid reaction of the SS prepolymer results in phase development more like that of a block copolymer system undergoing microphase separation. The high degree of connectivity between HS and SS sequences decreases the driving force for phase separation, and the rapid development of M_w (and hence viscosity) will impede molecular mobility and reduce the rate of phase separation, such that the system is essentially single phase until deep into the unstable region. The overall rate of reaction in RIM-PUr systems is very high and copolymerization proceeds rapidly, driving the system towards the two-phase equilibrium position (Eq). Microphase separation, however, lags well behind and at low values of T_{RIM} (i.e. low mould temperatures) vitrification arrests the process at a relatively early stage, resulting in a highly phase-mixed, brittle material which cracks upon demoulding[37,41]. Thus, commercial RIM-PUr systems utilize significantly higher mould temperatures (100–120°C) than comparable RIM-PUU systems (~70°C), which is equivalent to raising the coexistence curve with respect to the T_g curve, allowing a greater degree of microphase separation to occur prior to vitrification. For both RIM-PUU and PUr systems, higher SS functionality results in a more rapid development of copolymer molar mass with concomitant reductions in the degree of phase separation, as measured by d.s.c. D.m.t.a. reveals this reduction to be due to increased domain-boundary mixing, indicating a greater degree of phase connectivity. It is this increased connectivity which results in the significant improvements in green strength exhibited by both PUU and PUr materials, which may be likened to the increases in strength resulting from improved matrix–fibre bonding in composite materials.

CONCLUSIONS

During RIM copolymerization, significant variations in the development of molar mass and HS sequence length occurred. These variations were due either to unequal reactivity of the monomers or to changes in SS functionality, which markedly affected the development of copolymer structure as the system phase separated via spinodal decomposition. A statistical model of the copolymerization, based on recursive-method calculations, showed that both higher SS reactivity and SS functionality resulted in a more rapid development of copolymer molar mass. Consequently, increasing SS functionality was shown to increase significantly the incipient (green) strength of both PUU and PUr, but also to reduce the overall degree of phase separation developed in these materials (as determined by d.s.c. and d.m.t.a.), due to increased domain boundary mixing. Reactivity differences were shown to result in RIM-PUr which, because of their much greater SS reactivity than equivalent PUU systems, exhibited relatively poor green strength and a higher degree of phase-mixing. The kinetic competition between polymerization and phase separation processes was interpreted with reference to a phase diagram. In systems with low SS reactivity, such as PUU, phase development was shown to be more like that in a blend with HS homopolymerization, rapid macrophase separation (of unconnected HS and SS chains) being the favoured processes. Materials formed under these conditions will form relatively coarse, highly phase-separated co-continuous morphologies. However, in systems with high SS reactivity, such as PUr, the rapid reaction of the SS prepolymer resulted in phase development more like that of a block copolymer system undergoing microphase separation.

ACKNOWLEDGEMENTS

The authors would like to thank A. J. Ryan for his helpful discussions concerning RIM phase diagrams. The authors also wish to acknowledge the kind donation of the reactants used in this study from Lankro Chemical, Union Carbide Chemical, ARCO, Texaco Chemical, Lonza AG and Dow Chemical.

REFERENCES

1 Macosko, C. W. 'Fundamentals of Reaction Injecting Moulding', Hanser, Munich, 1989
2 Ryan, A. J. and Stanford, J. L. In 'Comprehensive Polymer Science' (Ed. G. Allen and J. C. Bevington), Pergamon Press, Oxford, 1988, Vol. 5, Ch. 25, p. 427
3 Ryan, A. J. *Polymer* 1990, **31**, 707
4 Ryan, A. J., Still, R. H. and Stanford, J. L. *Plast. Rubb. Proc. Appl.* 1990, **13**, 99
5 Willkomm, W. R. PhD Thesis, University of Minnesota, USA, 1990
6 Willkomm, W. R., Chen, Z. S., Macosko, C. W., Gobran, D. A. and Thomas, E. L. *Polym. Eng. Sci.* 1988, **28**, 888
7 Stanford, J. L., Wilkinson, A. N., Lee, D-K. and Ryan, A. J. *Plast. Rubb. Proc. Appl.* 1990, **13**, 111
8 Ryan, A. J., Stanford, J. L. and Still, R. H. *Polymer* 1991, **32**, 1426
9 Ryan, A. J., Stanford, J. L. and Birch, A. J. *Polymer*, 1993, **34**, 4874
10 Birch, A. J., Stanford, J. L. and Ryan, A. J. *Polym. Bull.* 1989, **22**, 629
11 Ryan, A. J., Stanford, J. L. and Still, R. H. *Brit. Polym. J.* 1988, **20**, 77
12 Macosko, C. W. 'Fundamentals of Reaction Injection Moulding', Hanser, Munich, 1989, Sec. 2.7
13 Camberlin, Y. and Pascault, J. P. *J. Polym. Sci. (Polym. Phys. Ed.)* 1984, **22**, 1835

14 Ryan, A. J., Stanford, J. L. and Still, R. H. *Polym. Comm.* 1988, **29**, 196
15 Critchfield, F. E. and Gerkin, R. M. *J. Elast. Plast.* 1976, **8**
16 Zdrahala, R. J. and Critchfield, F. E. In 'Reaction Injection Moulding and Fast Polymerization Reactions' (Ed. J. E. Kresta), *Polym. Sci. Tech.*, Plenum, 1982, **18**
17 Camargo, R. E., PhD Thesis, University of Minnesota, USA, 1984
18 Camargo, R. E., Macosko, C. W., Tirrell, M. and Wellinghoff, S. T. *Polymer* 1985, **26**, 1145
19 Camargo, R. E., Macosko, C. W., Tirrell, M. and Wellinghoff, S. T. In 'Reaction Injection Molding' (Ed. J. E. Kresta), *ACS Symp. Ser.* **270**, 1985
20 Nishimura, H., Kojima, H., Yarita, T. and Nishiro, M. *Polym. Eng. Sci.* 1986, **26**, 585
21 Lee, D-K. PhD Thesis, Victoria University of Manchester, 1988
22 Markovs, R. A. *J. Cell. Plast.* 1985, p. 326
23 Burchell, D. J. and Porter, J. R. *Proc. 32nd SPI Ann. PU Tech. Mark. Conf.*, 1989
24 Morgan, R. E., Berg, J. W. and Klumb, G. A. *Proc. 32nd SPI Ann. PU Tech. Mark. Conf.* 1989, 262
25 ASTM D1638M, American Society for Testing on Materials (standard)
26 Sorenson, W. R. and Campbell, T. W. 'Preparative Methods in Polymer Chemistry', Wiley Interscience, New York, 1981
27 Ogg, C. L., Porter, W. L. and Willits, C. O. *Ind. Eng. Chem. Ann. Ed.* 1945, **17**, 394
28 Wilkinson, A. N., PhD Thesis, Victoria University of Manchester, 1990
29 Camberlin, Y. and Pascault, J. P. *J. Polym. Sci. (Polym. Chem. Ed.)* 1983, **21**, 415
30 Lyne, J. PhD Thesis, Victoria University of Manchester, 1990
31 Saunders, J. H. and Frisch, K. C. 'Polyurethanes Chemistry and Technology Part 1', Interscience, New York, 1962, pp. 32–36
32 Woods, G. 'The ICI Polyurethanes Book', 2nd Edn., ICI/Wiley, 1990, pp. 35–39
33 Glasspool, J. Proc. of UTECH '86, The Hague, 1986, pp. 14–19
34 US patent, 3 654 370, Texaco Chemical Company, 1972
35 'Jeffamine' technical data sheet SC-024, Texaco Chemical Company, 1991
36 Birch, A. J. PhD Thesis, Victoria University of Manchester, 1991
37 Kirkland, C. *Plast. Tech.* 1986, **32**(3), 83
38 Leibler, L. *Macromolecules* 1980, **13**, 1602
39 Benoit, H. and Hadziannou, G. *Macromolecules* 1988, **21**, 1449
40 Pannone, M. C. MS Thesis, University of Minnesota, USA, 1985
41 Dominguez, R. J. G., Rice, D. M. and Grigsby, R. A. *Plast. Eng.* Nov. 1987
42 Lopez-Serrano, F., Castro, J. M., Macosko, C. W. and Tirrell, M. *Polymer* 1980, **21**, 263
43 Pannone, M. C. and Macosko, C. W. *Polym. Eng. Sci.* 1988, **28**, 660
44 Wang, K. J., Huang, Y. J. and Lee, L. J. *Polym. Eng. Sci.* 1990, **30**, 654
45 Flory, P. J. 'Principles of Polymer Chemistry', Cornell Press, Ithaca, 1953
46 Callister, S., Keller, A. and Hikmet, R. M. *Makromol. Chem., Makro. Symp.* 1990, **39**